Supporting Information for:

Transformation of Hexahydro-1,3,5-trinitro-1,3,5-triazine (RDX) by Permanganate

CHANAT CHOKEJAROENRAT [†], STEVE D. COMFORT [‡,*], CLIFFORD HARRIS [§], DANIEL D. SNOW [||], DAVID CASSADA [||], CHAINARONG SAKULTHAEW [‡], AND TUNLAWIT SATAPANAJARU [⊥]

* Corresponding author phone: 402-472-1502; fax: 402-472-7904; e-mail: scomfort@unl.edu.

[†] Department of Civil Engineering, University of Nebraska-Lincoln

[‡] School of Natural Resources, University of Nebraska-Lincoln

[§] Department of Chemistry, Albion College, MI

[||] Water Science Laboratory, University of Nebraska-Lincoln

⊥ Department of Environmental Science, Kasetsart University, Bangkok, Thailand

Contents

SI-1. Additional Experimental Section
Figs. S1; S2
SI-2. RDX Purification
SI-3 Experimental Controls
Fig. S3; Table S1; Figs. S4; S5
SI-4. Effect of quenching agents on RDX degradation products
Figs. S6; S7; S8
SI-5. RDX Batch Experiments (Autocatalysis of permanganate)
Figs. S9; S10
SI-6. Kinetic Models
Figs. S11; S12; S13; S14
SI-7. Temperature dependency
Table S2
SI-8 Single electron transfer versus hydride (or hydrogen) atom removal
Fig. S15; S16; S17
SI-9. Proposed RDX degradation via proton abstraction
Fig. S18
SI-10. References

SI-1. Additional Experimental Section

Chemical Standards. Commercial-grade RDX (~90% purity) was obtained from the Fort Detrick U.S. Biomedical Research and Development Laboratory (Frederick, MD). 4-nitro-2,4-diazabutanal, (4-NDAB, >99% purity) was custom synthesized by SRI International (Menlo Park, CA). Sodium permanganate ($NaMnO_4$, 40% by weight) and potassium permanganate ($KMnO_4$) were obtained from Fisher Scientific (Pittsburgh, PA). Reagent grade hydrogen peroxide (H_2O_2, 30% v/v), methanol, manganous sulfate ($MnSO_4 \bullet H_2O$) (J.T.Baker, Phillipsburgh, NJ), and manganous carbonate ($MnCO_3$, 99.9%, metals basis) (Alfa Aesar, Ward Hill, MA) were used as purchased. All solvents used in this research were HPLC grade (Fisher Scientific, Springfield, NJ). An analytical RDX standard (100 μg/mL) in a 50:50 acetonitrile-methanol matrix was purchased from AccuStandard (New Haven, CT). Nitrate (NO_3^-), Ammonium (NH_4^+) (1000 mg/L, GFS Chemicals, Columbus, OH) and nitrite (NO_2^-) (1000 mg/L, Absolute Standards Inc., Hamden, CT) standards were used as purchased. Nitrous oxide (N_2O) standards were prepared from the 2% stock gases (mole basis) obtained from Scott Specialty Gases (Plumsteadville, PA).

High-Performance Liquid Chromatography (HPLC). Temporal changes in RDX and degradate concentrations were quantified at a 220 nm by HPLC equipped with a photodiode array detector (Shimadzu Scientific Instruments, Columbia, MD). Peak separations were performed by injecting 20 μL of sample into a Supelcosil LC-8, 250 x 4.6 mm, (Supelco, Sigma-Aldrich Corporation, PA) or a Fluophase PFP perfluorinated column, 250 x 4.6 mm, coupled with a guard column (Thermo Scientific, MA). A variety of mobile phases and flow rates (0.50-1.50 mL/min) were tested to separate peaks but the typical mobile phase was an isocratic mixture of methanol and H_2O (30:70), or acetonitrile and H_2O (50:50) at a flow rate of 0.75 mL/min.

Ion Chromatography (IC). Analysis of NO_2^-/NO_3^- and NH_4^+ were performed with a Dionex DX-120 Ion Chromatograph (Sunnyvale, CA) with suppressed conductivity detection (conductivity detector, CDM-3). For anion analysis, separation was performed with an AS-15 IonPac column, 250 x 4.0 mm, using an eluent of 38 *m*M NaOH at a flow rate of 1 mL/min. For cation analysis, separation was performed with a CS12A IonPac column, 250 x 4.0 mm, using an isocratic eluent of 5.5 *m*M H_2SO_4 at a flow rate of 1.2 mL/min. The injection volume for both analyses was 25 μL. To effectively analyze samples by IC, RDX samples treated with MnO_4^- were quenched with $MnCO_3$.

Gas Chromatography/Electron Capture Detector (GC/ECD). Nitrous oxide (N_2O) emitted from the RDX-MnO_4^- reaction was measured by direct injection into a Hewlett-Packard (Palo Alto, CA) 6890 GC operated with a HP-Plot column (Molecular sieve 5A) 30 m/0.53 mm (50 μm film thickness) and electron capture detector (ECD). A P-5 gas (a mixture gas of 95% Argon and 5% CH_4) was used as a carrier gas for the GC system. The GC oven was equilibrated at least two hours at 225°C before analysis.

UV-Spectrophotometer. Changes in MnO_4^- concentrations were monitored by diluting solution with Ultra Pure water in 20-mL vials and quantifying concentrations with a HACH Spectrophotometer DR2800 (HACH Company, Loveland, CO) at a wavelength of 525 nm. A test of whether colloidal MnO_2 interfered with quantification of MnO_4^- is presented in SI-3.

Analysis of N-containing gases.

Nitrogen Gas (N_2) To determine if N_2 gas was a product of the RDX-MnO_4^- reaction, experiments were conducted under vacuum in a Rittenburg tube, a two-legged Y-shaped tube (Fig. S1), containing crystalline RDX (both ^{14}N-RDX and ^{15}N-RDX) in one side and concentrated MnO_4^- solution in the other. Uniformly labeled, [U-^{15}N]RDX, (^{15}N abundance of 97 atom%) was purchased from PerkinElmer (Waltham, MA). Prior to starting the reaction (i.e., mixing), all gases were evacuated through a vacuum line

while the MnO_4^- solution was simultaneously frozen. Once the frozen solution melted, we mixed it with the crystalline RDX in the other side. The tube was then immersed in water (~20°C) to confirm no leakage and avoid atmospheric gas contamination. We also mirrored this experiment without vacuuming so as to monitor the RDX concentration by HPLC. When RDX was completely degraded, gas emission was drawn by a vacuum system passing through a cold trap to freeze all gases but N_2 gas (Fig. S2; (*1*)). Gas samples were then collected in sample bulb and cryogenically transferred to an Optima Dual Inlet mass spectrometer (VG Isotech, Colchester, VT).

Results indicated that no increase in gas pressure was observed during the sample transfer and full scan measurement showed that, very little, if any N_2 gas (*m/z* = 28, 29, 30) formed during treatment. The primary reaction gas formed, N_2O, was trapped in the preparation line but was not analyzed on the instrument.

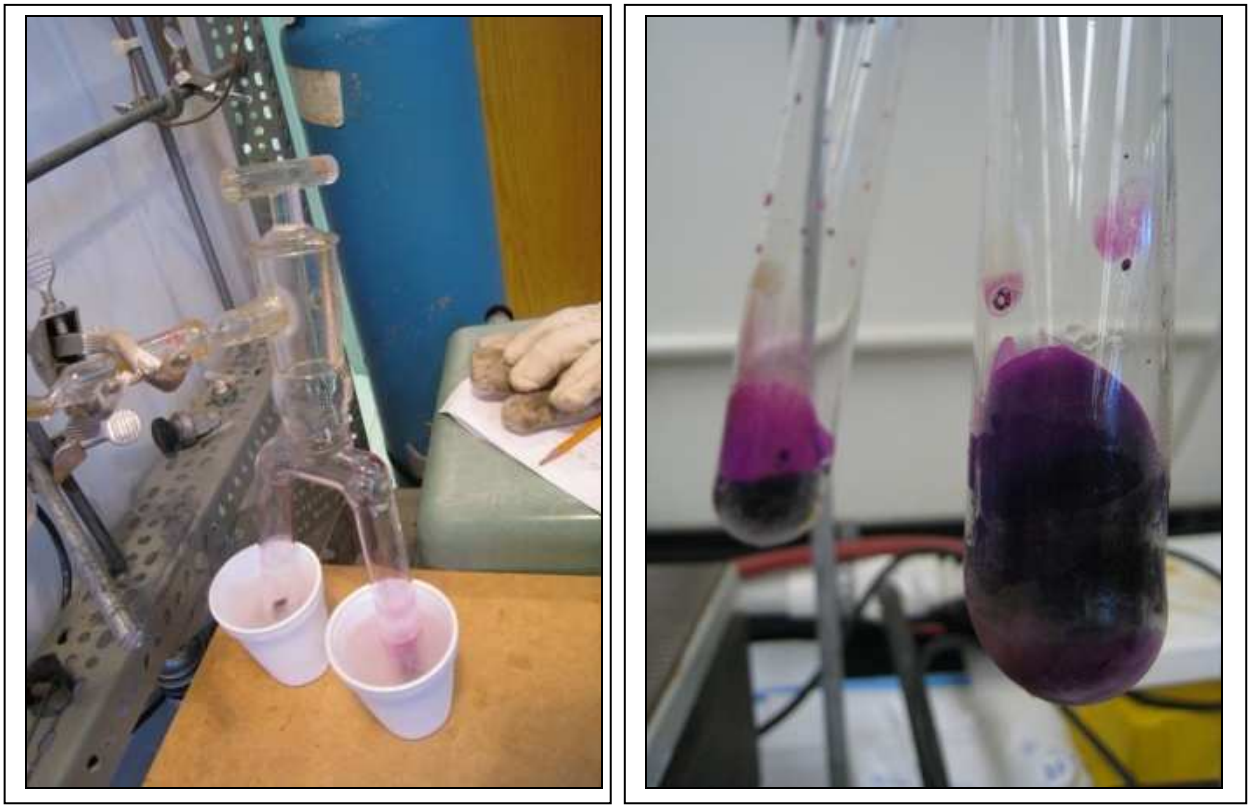

Figure S1: (Left) The Rittenburg tube containing MnO_4^- solution was frozen in liquid nitrogen while all gases were being vacuumed. (Right) thawed RDX- MnO_4^- solution after mixing.

Figure S2: Experimental system for trapping of N_2 gas. When RDX was completely degraded, all gases were evacuated from the Rittenburg tube (Lower Circle) and trapped in the vacuum system except N_2 gas which was forced to the gas-tight sampling tube (Upper Circle).

NO_x gases (i.e., NO_2 and NO) Besides the N_2 and N_2O gases, we also investigated the production of NO_x gases (i.e., NO_2 (nitrogen dioxide) and NO (nitric oxide)) to determine if they were released during the RDX-MnO_4^- reaction. NO_2 is known to produce from the reaction of concentrated nitric acid and copper and is a toxic brownish gas with a pungent acid odor. However, in the diluted solution of nitric acid and copper, water molecules cause the reaction to produce NO instead. Although we did not observe a distinct brownish color of NO_2 during the RDX- MnO_4^- reaction, we attempted to identify NO_2 and other possible transformation products by treating 5 mL of

saturated RDX (12.1 mg ^{15}N-labeled and 0.4 mg non-labeled RDX) with 168.067 *m*M of MnO_4^- in a 12-mL vial with a gastight septum. Each vial was degassed for 5 min and purged with Helium for 5 min by the acid injector (3.2 psi, Gilson, Middleton, WI) at a flow rate of 20.5 mL min^{-1}. $NaMnO_4$ (0.2 mL of 40% by weight) was injected into a vial by a gastight syringe. The temperature was controlled in a Precision 180 Series water bath at 60℃ (Precision Scientific Co., Baltimore, MD) to increase RDX destruction rate. At 11 d, a 10 µL gas sample was removed from the vial and injected directly into a Hewlett-Packard 5890 GC (Palo Alto, CA) an Agilent 5972 quadrupole mass spectrometer. The N gases were separated on a 30 m/0.32 mm PLOT Moleseive column (J&W Scientific, Folsom, CA). The instrument was calibrated using Helium reference gas.

Results indicated that NO_2 and NO were not detectable during the RDX-MnO_4^- reaction. A complicating factor, however, is that if NO_x gasses (i.e., NO or NO_2) are liberated during the treatment of RDX with MnO_4^-, it will be difficult to quantify because MnO_4^- provides an excellent means of removing NO by oxidizing it to NO_2^- and NO_3^-, depending on pH (*2-4*). Alkaline or acidic MnO_4^- has also been shown to be capable of trapping NO_x gas emission from soils (*5-8*).

202 **SI-2. RDX Purification**

203 The commercial grade RDX contains ~90% RDX and ~10% HMX (octahydro-
204 1,3,5,7-tetranitro-1,3,5,7-tetrazocine). To remove interferences and degradation artifacts
205 associated with HMX, we removed the HMX by preparing a concentrated RDX solution
206 (in acetonitrile) and purified to ≥99% RDX by using a Waters 2695 HPLC (Waters Corp.,
207 Milford, MA) with a temperature-controlled (30℃) Kromasil C18 column, 250 x 4.6 mm,
208 (Thermo Scientific, MA) and Photodiode Array Detector (Waters 2996, Waters Corp.,
209 Milford, MA). The flow rate for this purification procedure was 1.5 mL/min with a
210 repeated injection volume of 25 μL. A mobile phase of methanol (in H_2O) was used with
211 the following gradient: 60:40 for 9 min followed by 90:10 for 3.5 min and 60:40 for the
212 remainder of the run (~7.5 min). A Spectrum CF-2 fraction collector was used to isolate
213 the RDX peak eluting from the column. The RDX fractions were combined and
214 concentrated by the RapidVap evaporation system (Labconco, Kansas city, MO) in
215 which a cylindrical receptacle was swirled and blown by N_2 gas at 50℃ until dry.
216
217
218
219
220
221
222
223
224
225
226
227

SI-3. Experimental Controls

A series of experiments were performed under batch conditions to verify that RDX destruction rates by MnO_4^- were similar when the initial pH was controlled or allowed to drift as the reaction proceeded (Fig. S3), the use of $MnCO_3$ as a quenching agent did not significantly influence sample pH or temperature (Table S1), RDX concentrations after quenching with $MnCO_3$ were stable and not subject to hydrolysis (Fig. S4), and that quantification of MnO_4^- concentrations were not influenced by colloidal MnO_2 (Fig. S5).

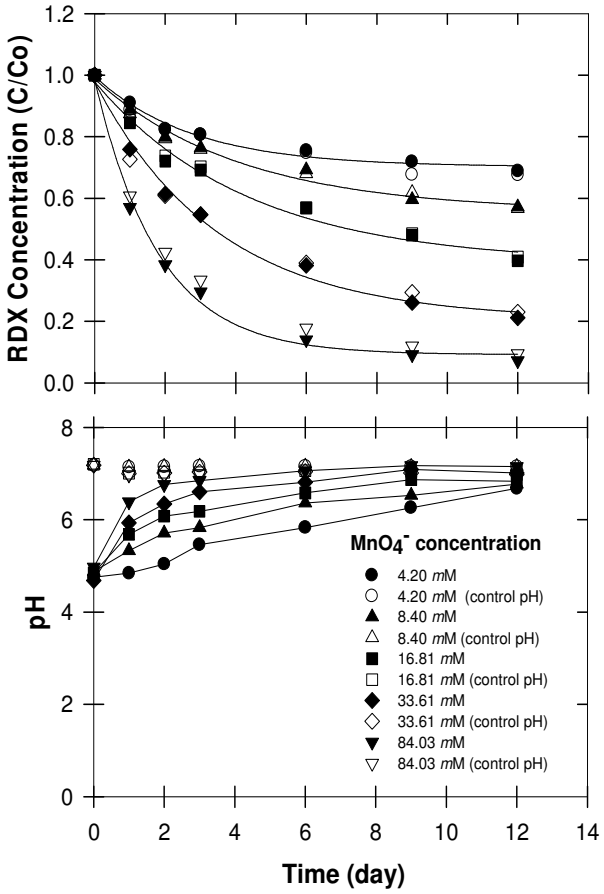

Figure S3. Changes in RDX concentration and pH by various concentrations of MnO_4^- under controlled and unbuffered pH.

Table S1. Changes in pH and temperature of RDX-MnO_4^- solution following quenching with various mass of $MnCO_3$.

$MnCO_3$ (g per mL of sample)	pH before quenching	pH after quenching	Temp before quenching (℃)	Temp after quenching (℃)
0.00 g	5.88		25	
0.03 g	5.82	6.15	25	24
0.04 g	5.81	6.02	25	23
0.05 g	5.85	6.02	25	23
0.06 g	5.80	5.93	25	23
0.07 g	5.74	5.86	25	22.5

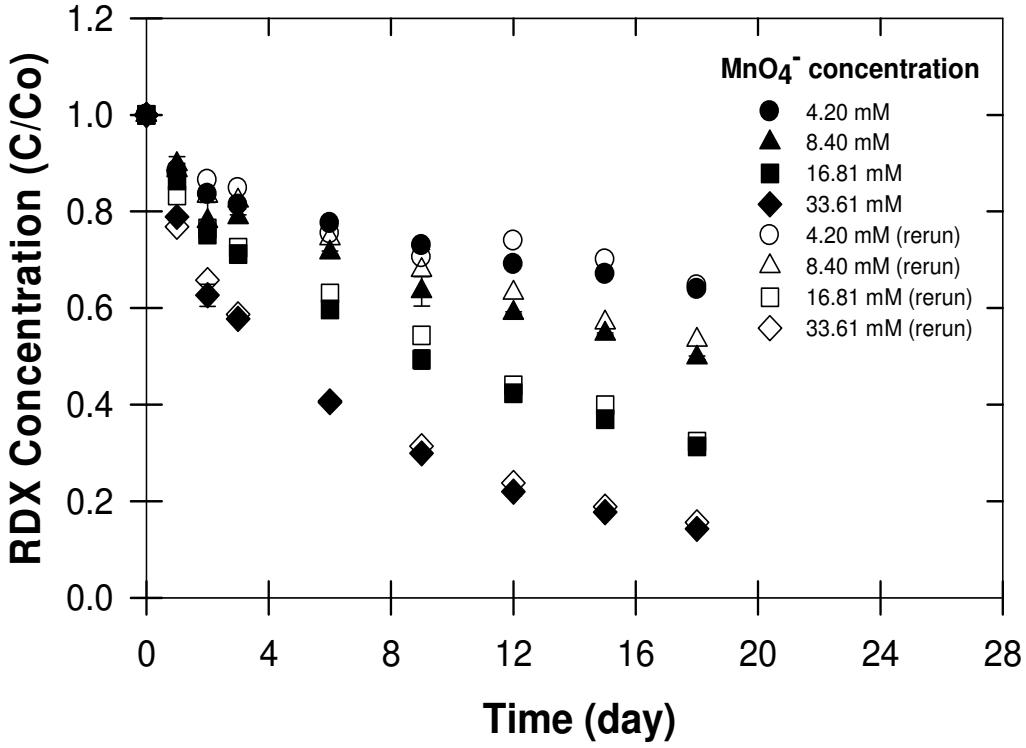

Figure S4. Temporal changes in RDX concentrations following treatment with varying MnO_4^- concentrations. Solid symbols signify concentrations of samples analyzed immediately, open symbols are the same samples analyzed 9 d later.

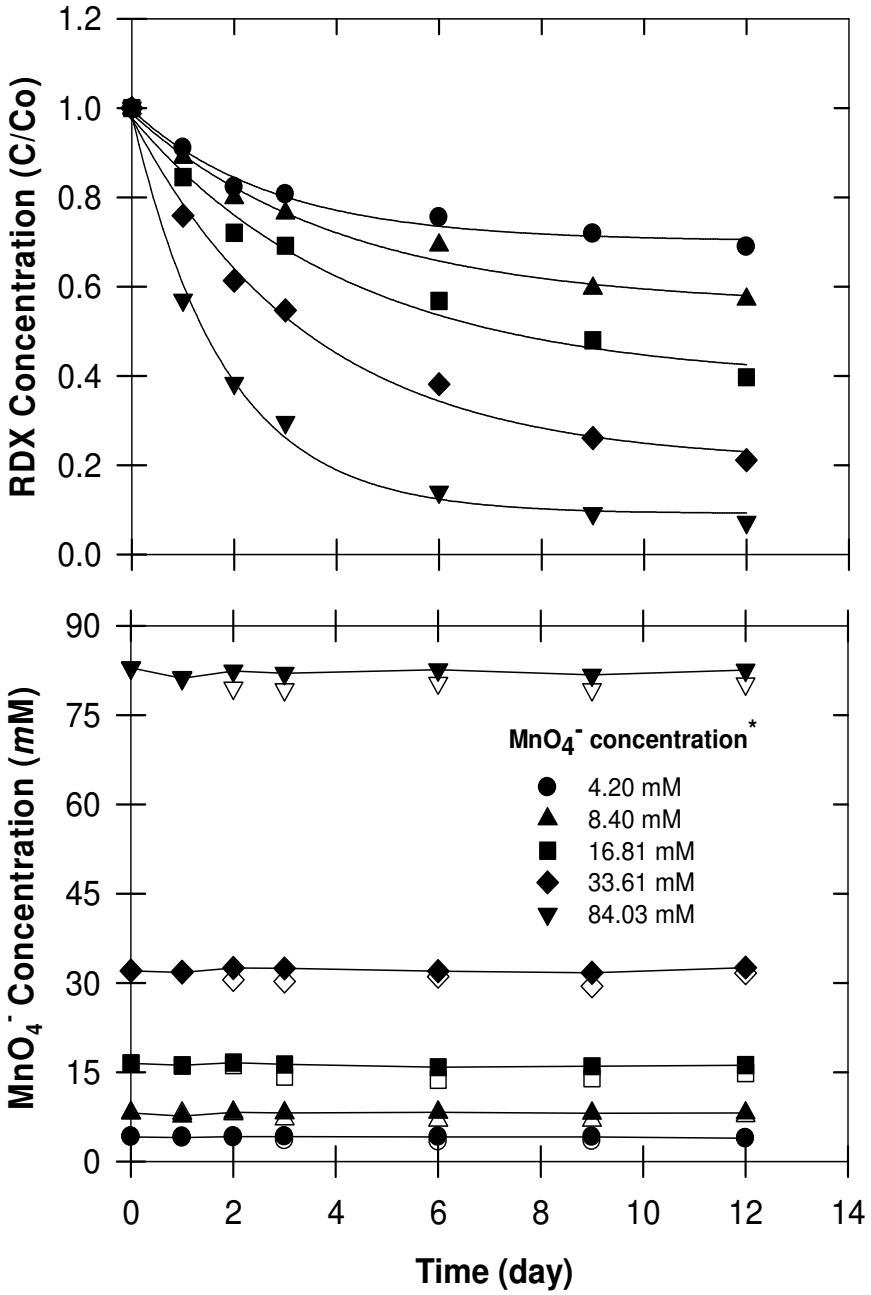

Figure S5. Changes in RDX and MnO_4^- concentrations following treatment with varying MnO_4^- concentrations. Solid symbols indicate MnO_4^- concentrations determined without filtration, open symbols with filtration (0.45μm glasswool filter).

321

322 **SI-4. Effect of quenching agents on RDX degradation products**

323 To determine the effect of quenching agents on RDX degradation products,
324 aqueous solutions of RDX (0.07 *m*M) were treated with 33.61 *m*M of MnO_4^-. We initially
325 prepared RDX solutions by spiking 150 mL H_2O with 1.04 mL of RDX stock solutions
326 prepared in acetone but the acetone-MnO_4^- reaction resulted in autocatalysis of MnO_4^-
327 at alkaline pH and prevented further degradation of RDX >10 d (see Supporting
328 Information; SI-5). Consequently, all aqueous RDX solutions were prepared by
329 dissolving purified crystalline RDX in water over several days. Once MnO_4^- was added
330 to RDX solutions to initiate the reaction, samples were periodically collected and
331 quenched with $MnCO_3$ or H_2O_2. Quenching with $MnCO_3$ (pH = 6.7) was performed as
332 described in the main manuscript. When quenched with 30% H_2O_2 (0.04 mL per mL of
333 sample), samples were required to mix continuously to control H_2O_2 consumption. The
334 pH of samples quenched with H_2O_2 were found to increase significantly (pH = 11.5). To
335 elucidate this pH effect, one set of batch samples were quenched with $MnCO_3$, and we
336 increased the pH to that observed with the H_2O_2 by adding NaOH. Temporal changes in
337 RDX, 4-nitro-2,4-diazabutanal (4-NDAB), NO_3^-, and NO_2^- concentration were monitored
338 by using HPLC and IC.

339 Results indicated that an RDX solution treated with MnO_4^- led to complete RDX
340 transformation within 15 d (Fig. S6A). To quantify temporal changes in RDX
341 concentrations, samples were removed from the batch reactors every 2 to 3 d and
342 chemically quenched to remove MnO_4^- and prevent further RDX oxidation. While
343 $MnSO_4$ is commonly used as a quenching agent (*9-13*) and does not interfere in HPLC
344 analysis of RDX (*12-13*), the sulfate liberated interferes with NO_2^- and NO_3^- analyses by
345 ion chromatography (IC). By using $MnCO_3$, we avoided this interference during IC
346 analysis. However, the disadvantage of using $MnCO_3$ is that, at the concentrations of

quenching agents used, $MnCO_3$ takes longer than $MnSO_4$ to quench the MnO_4^-. Given the typical time course of the batch experiments (15 d), we compared RDX destruction rates from the same batch experiment and observed similar RDX destruction rates (Fig. S7).

Another consideration is that the quenching agent can alter the pH of the sample and possibly influence product formation or stability. When samples were quenched with $MnSO_4$, solution pH decreased from ~7.2 (before quenching) to pH 2.6 after quenching as predicted by the following reaction (Eq. S1).

$$2NaMnO_4 + 3MnSO_4 + 2H_2O \rightarrow 2Na^+ + 3SO_4^{2-} + 4H^+ + 5MnO_2 \qquad \text{[Eq. S1]}$$

When RDX-MnO_4^- solutions were quenched with $MnCO_3$ (Eq. S2), sample pH (after quenching) remained near 6.7, which is closer to the pH of the unquenched RDX-MnO_4^- solution.

$$2NaMnO_4 + 3MnCO_3 + 2H_2O \rightarrow 2Na^+ + 3HCO_3^- + 5MnO_2 + H^+ \qquad \text{[Eq. S2]}$$

Product analysis during the RDX-MnO_4^- reaction showed that when $MnCO_3$ was used as a quenching agent, we observed NO_3^- production in the reaction but no NO_2^- and only a trace of 4-NDAB (~0.004 *m*M) (Fig. S6A).

Peroxide was also used as a quenching agent. Here, peroxide reacts with MnO_4^- by the following reaction (Eq. S3):

$$2NaMnO_4 + 4H_2O_2 \rightarrow 2Na^+ + 2OH^- + Mn_2O_3 + 3H_2O + 4O_2 \qquad \text{[Eq. S3]}$$

Because OH^- is liberated, the pH of samples quenched with H_2O_2 increased (pH

373 ~11.5) and we observed NO_2^-, NO_3^-, and 4-NDAB (Fig. S6B). Although the magnitude of
374 NO_3^- generated was similar to what we observed when $MnCO_3$ was used as a
375 quenching agent (Fig. S6A, S6B), RDX destruction kinetics were much faster (k = 1.83
376 d^{-1}). Because we suspected excess peroxide may have contributed to RDX destruction,
377 we conducted an experiment where RDX solution was treated with H_2O_2 in the same
378 ratio as used in quenching process (0.04 mL of 30% H_2O_2 to 1 mL RDX or 1.2% (v/v)
379 H_2O_2; no MnO_4^-). Results showed that RDX concentration was not significantly affected,
380 pH remained constant, and RDX degradation products (NO_2^- NO_3^-, and 4-NDAB) were
381 not observed.

382 The peroxide concentration used in this control experiment (RDX + H_2O_2 only)
383 was higher than what the quenched RDX-MnO_4^- samples would have experienced
384 because most, if not all, of the H_2O_2 would have reacted with the MnO_4. Therefore, the
385 increased RDX destruction kinetics observed (Fig. S6B) does not appear to be directly
386 related to the presence of excess peroxide. Rather, catalytic decomposition of H_2O_2 into
387 various radicals (i.e., superoxide anion (O_2^-), hydroperoxide radical (HO_2•), and hydroxyl
388 radical (•OH)) may have played a role in the enhanced degradation of RDX (Fig. S6B).
389 Although MnO_2 surfaces can enhance oxidation reactions (*14*), this precipitate, which
390 forms during RDX-MnO_4^- reaction (*12*), is also a catalyst for decomposition of H_2O_2 and
391 both O_2^- and HO_2• are favored at high pH (*15-16*). O_2^- itself is known to be capable of
392 degrading RDX (*17*). Furthermore, during the quenching process, Mn_2O_3 is liberated
393 (Eq. S3) and can simultaneously act as a catalyst for degradation of organic compounds
394 in the presence of H_2O_2 (*15, 18*). Another possibility is that the alkaline pH created
395 during the quenching process (Eq. S3) facilitated H_2O_2 decomposition into •OH which
396 contributed to RDX degradation. Moreover, Gates-Anderson et al. (*19*) observed that in
397 strongly basic solutions (pH > 9) •OH can also be generated from MnO_4^- and directly
398 oxidize organic contaminants. These explanations support a seven-fold increase of

RDX destruction kinetics (Figs. S6A, S6B).

Finally, an elevated temperature may also have been responsible for greater RDX destruction in the H_2O_2 quenched samples. Heilmann et al. (*20*) showed that alkaline hydrolysis rates of RDX in aqueous solution dramatically increased at high temperature (50°C). We observed that using H_2O_2 as a quenching agent caused a rapid 9°C increase in sample temperatures. Because H_2O_2-MnO_4^- reaction is exothermic, it is reasonable that the combination of alkaline pH and heat may have contributed to RDX degradation (See also *Effect of Temperature on RDX-MnO_4^- Reaction* in the main manuscript).

Given that the treatment of RDX with peroxide alone did not cause an increase in pH or the production of NO_2^- and 4-NDAB, the alkaline pH created by the H_2O_2-MnO_4^- reaction was likely responsible for the degradation products observed. To test this further, we again used $MnCO_3$ as a quenching agent and artificially raised the pH of the samples before and after quenching to pH 11.5 (similar to what was observed with H_2O_2 as a quenching agent). Results showed RDX degradation was slower than when peroxide was used to quench the MnO_4^- and closer to the results obtained when $MnCO_3$ was used without pH adjustment (Fig. S6A, k = 0.26 d^{-1}; Fig. S6C, k = 0.33 d^{-1}). This observation lends credence to the possibility that peroxide radicals may have been involved during the quenching of MnO_4^- with H_2O_2 (Fig. S6B). Using $MnCO_3$ + alkaline pH also produced NO_2^- and 4-NDAB as reaction products (Fig. S6C). Two known RDX degradation schemes involve the removal of one nitro group (denitration) with the intermediate methylenedintramine (MEDINA) or two nitro groups and the formation of 4-NDAB (e.g. (*21*)). Thus, the detection of nitrite during the RDX-MnO_4^- reaction (with H_2O_2 quenching agent or $MnCO_3$ + alkaline pH) is likely a result of the alkalinity stabilizing NO_2^- and preventing further transformation. Numerous reports have shown

that nitrite is more persistent at alkaline pH (*22-23*). Balakrishnan et al. (*24*) also found NO_2^- as an endproduct of RDX hydrolysis.

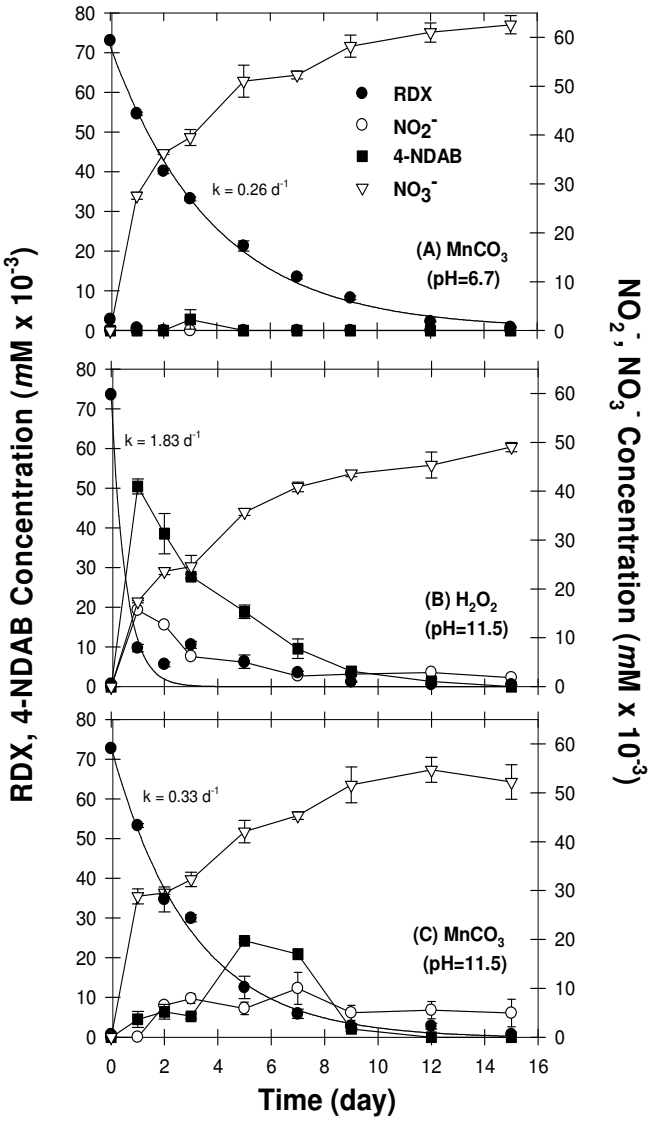

Figure S6: Changes in RDX concentration and production of degradation products (4-NDAB, NO_2^-, and NO_3^-) when quenched with; (A) 0.10 g $MnCO_3$ (per mL); (B) 0.04 ml 30% H_2O_2 (per mL, pH ~ 11.5); and (C) 0.10 g $MnCO_3$ (per mL) in which sample solutions pH was raised to 11.5 before and after quenching. Bars indicate sample standard deviations (n = 3).

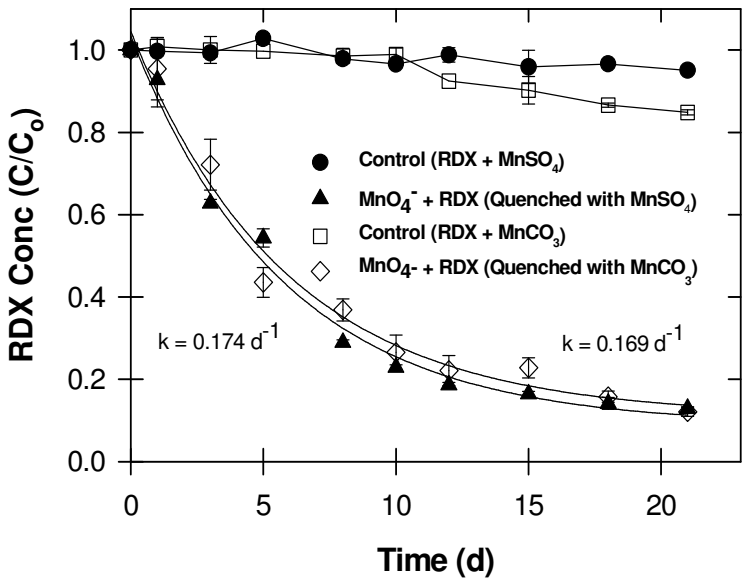

Figure S7: Comparison of RDX degradation kinetic rates when quenched with $MnSO_4$ or $MnCO_3$. Bars indicate sample standard deviations (n = 3).

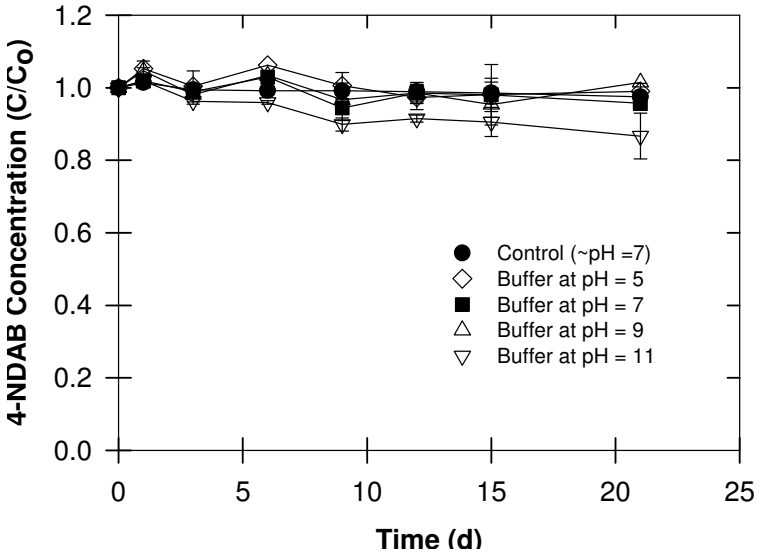

Figure S8: The effect of pH on 4-NDAB stability. Bars indicate sample standard deviations (n = 3).

476 **SI-5. RDX Batch Experiments (Facilitated Decomposition of permanganate)**

477 To evaluate the effects of initial MnO_4^- concentration on RDX destruction rates,
478 we conducted the batch experiment by treating 150 mL of aqueous ^{14}C-RDX (0.02 *m*M,
479 30000 dpm mL^{-1}, uniformly ring-labeled) and varying MnO_4^- concentration from 8.40 *m*M
480 to 168.07 *m*M. Each MnO_4^- concentration was replicated three times. Temporal samples
481 were periodically collected and quenched with $MnSO_4$ as described in analytical section
482 and monitored for the loss of RDX by HPLC and ^{14}C-activity by Liquid Scintillation
483 Counter (LSC).

484 Results indicated that treating aqueous (i.e., distilled water) RDX with 168.067
485 *m*M of MnO_4^- reduced RDX concentrations to zero within 10 d (k = 0.49 d^{-1}) (Fig. S9A).
486 Lower MnO_4^- concentrations (8.40-42.02 *m*M) reduced RDX destruction rates and
487 overall removal. For instance, when RDX was treated with 8.40 *m*M of MnO_4^-
488 destruction rates decreased ~70% (k = 0.14 d^{-1}) and only 29% of the initial RDX was
489 removed within 10 d (*25*). These results are similar to those reported by Adam et al.
490 (*12*) but differ in that temporal decrease in both RDX and ^{14}C concentrations (Fig. S9B)
491 reached a plateau after ~10 d. The reasons MnO_4^- failed to continually transform and
492 mineralize RDX beyond 10 d was investigated by monitoring temporal changes in pH
493 and MnO_4^- concentrations.

494 By repeating the experiment with 84.03 *m*M of MnO_4^- and monitoring MnO_4^- and
495 pH (Fig. S10A, S10B, S10C), we observed an increase in pH from 6.5 to > 8. Using
496 higher MnO_4^- concentrations (126.05, 168.07 *m*M) also produced similar changes in pH.
497 This increase in pH coincided with a significant decrease in MnO_4^- concentration (Fig.
498 S10B). By contrast, when a pH-stat (Metrohm Titrino 718S; Brinkman Instruments,
499 Westbury) maintained the pH at 7, RDX concentrations did not plateau but continued to
500 decrease and very little consumption of MnO_4^- was observed (Fig. S10A, S10B). It is
501 clear that in the unbuffered treatment, the rapid decrease in MnO_4^- concentration

502 coincided with the lack of further RDX destruction beyond 7 d (i.e., plateau). We believe
503 the loss of MnO_4^- was likely caused by a facilitated decomposition of permanganate at
504 alkaline pH. But alkaline pH alone was not solely responsible for the loss of MnO_4^-.
505 Adam et al. (*12*) evaluated the effect of pH on RDX destruction kinetics and reported no
506 pH effect in the range 4.1 to 11.3. A comparison of procedures used by Adam et al. (*12*)
507 and our protocol revealed that a higher percentage of acetone was used in our batch
508 reactors. This occurred by using RDX stock solutions prepared in acetone (both
509 unlabeled and ^{14}C-labeled) to spike the aqueous solutions with RDX. Although the
510 volume of acetone spiked into the aqueous batch reactors was relatively low (1.04 mL
511 acetone/150 mL H_2O), when this same concentration of acetone was added to 84.03
512 *m*M of MnO_4^- without RDX, a similar decrease in MnO_4^- was observed (Fig. S10D,
513 S10E, S10F); similarly, when aqueous RDX solutions were prepared without acetone,
514 the pH remained constant (Fig. S10F) and MnO_4^- consumption was negligible (Fig.
515 S10E). The plateau in RDX loss observed (Figs. S9, S10) resulted from the reaction of
516 acetone with MnO_4^- and likely included the oxidation of acetone to oxalic acid and the
517 reaction of oxalic acid with MnO_4^- to form Mn^{2+}, which is known to facilitate the
518 decomposition of MnO_4^-.
519 While the accelerated removal of MnO_4^- was traced back to the use of acetone
520 and subsequent formation of carboxylic acids in our batch reactors (Fig. S10), the
521 implications of this observation may be more than just an experimental anomaly. Oxalic
522 acid is a product of the TCE-MnO_4^- reaction (*26*). Li et al. (*27*) also showed that oxalate
523 was a primary oxidation product of the explosive TNT (2,4,6-trinitrotoluene) during
524 treatment with Fe^{2+} and H_2O_2 (i.e., Fenton oxidation). Thus, situations may arise where
525 oxalate (or other carboxylic acids) are present and cause excessive MnO_4^-
526 decomposition if the pH is not monitored and prevented from becoming alkaline.
527

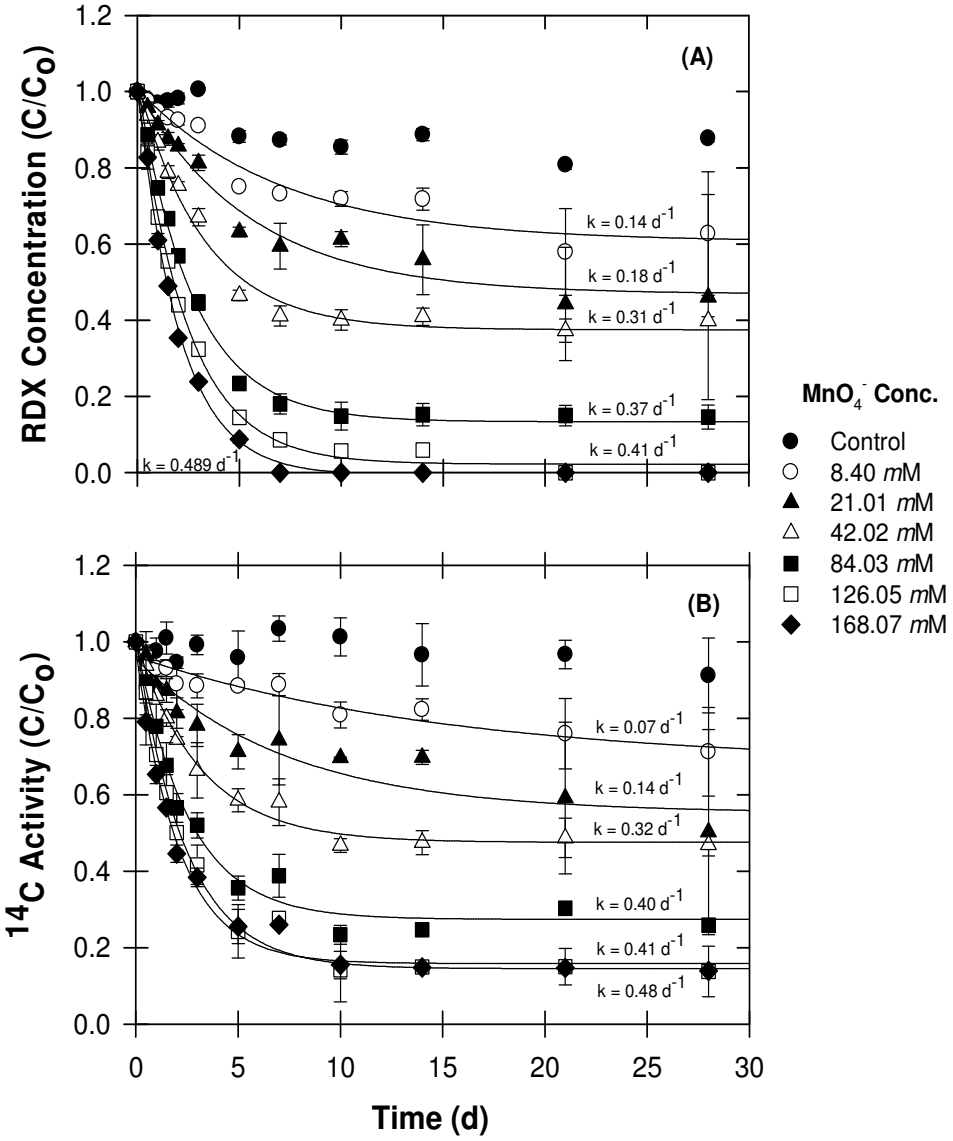

Figure S9: Loss of RDX and ^{14}C-activity in aqueous solution treated with various concentrations of MnO_4^-. Solution samples were quenched with $MnSO_4$. Bars indicate sample standard deviations (n = 3).

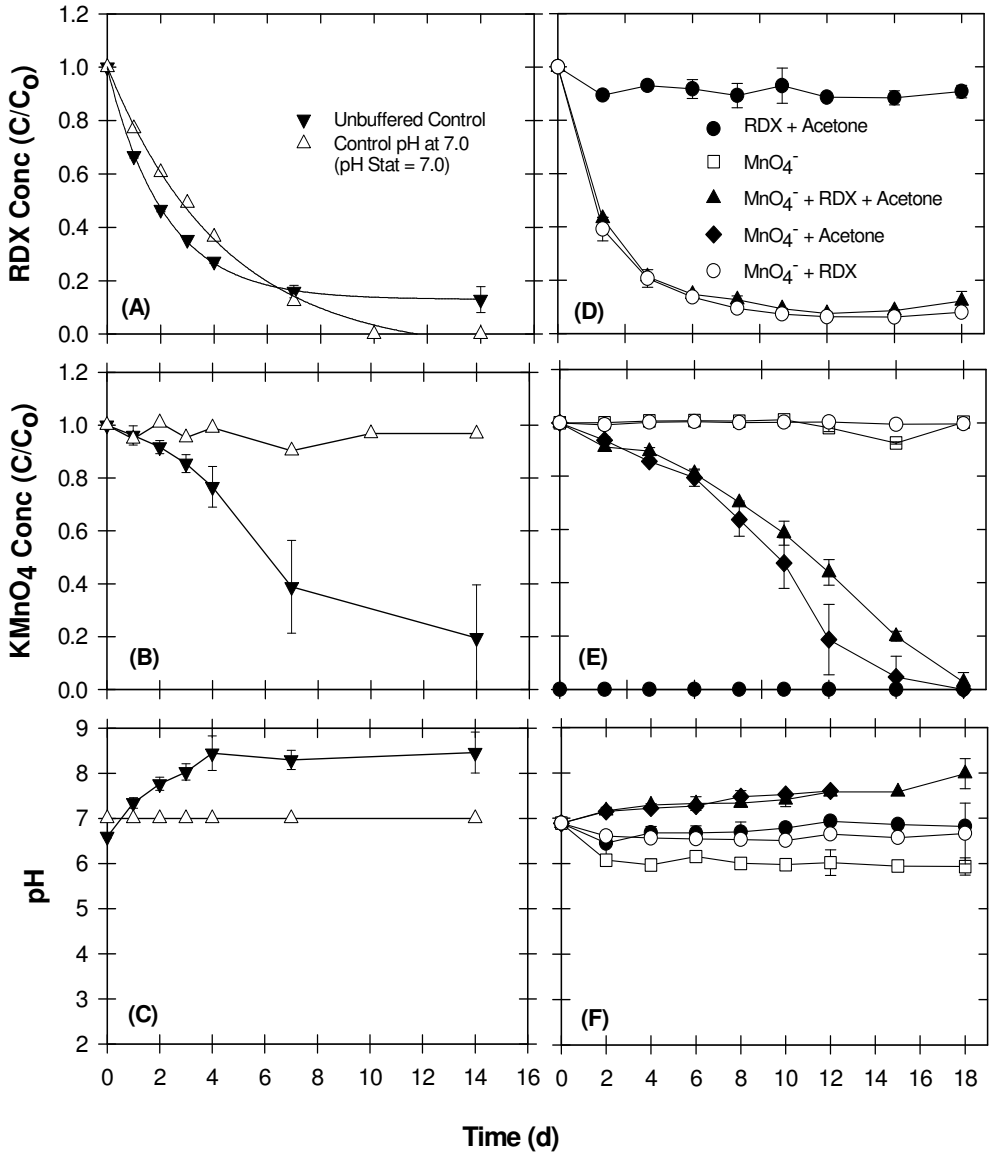

Figure S10: (A-C) Changes in RDX, MnO_4^- concentration, and pH in the presence of acetone following treatment with 84.03 *m*M of MnO_4^- (i.e., Unbuffered control, and control pH at 7). (D-F) Changes in RDX, MnO_4^- concentration, and pH with/without acetone. Solution samples were quenched with $MnSO_4$. Bars indicate sample standard deviations (n = 3).

SI-6. Kinetic Models

While second-order expressions are commonly used to describe contaminant destruction rates by MnO_4^- (*28-32*), if MnO_4^- is in excess, the reaction can also be described by a pseudo first-order expression (*12, 33*). Like many other second-order reactions between contaminant and MnO_4^-, the general rate equation can be written as:

$$r = -\frac{1}{\propto}\frac{d[RDX]}{dt} = k\,[RDX]^{\propto}[MnO_4^-]^{\beta} \qquad \text{[Eq. S4]}$$

$$r = k_{obs}\,[RDX]^{\propto} \qquad \text{[Eq. S5]}$$

$$k_{obs} = k\,[MnO_4^-]^{\beta} \qquad \text{[Eq. S6]}$$

Where $\propto$ is a reaction order with respect to RDX, β is a reaction order with respect to MnO_4^-, r is a reaction rate, k is a second-order rate constant, and k_{obs} is a pseudo-order rate constant. By varying the initial concentration of MnO_4^- and measuring k_{obs} by fitting the results into a pseudo first-order equation by regression analysis using computer software SigmaPlot Version 10.0 (*34*), the value of β with respect to MnO_4^- can be obtained by a log-log form of Eq. S6:

$$log\ k_{obs} = log\,k + \beta\,log\ [MnO_4^-]_o \qquad \text{[Eq. S7]}$$

Likewise, by varying the initial concentration of RDX and measuring the reaction rate, the value of $\propto$ with respect to RDX can be determined by a log-log form of Eq. S5. To evaluate for the reaction rates, we used the initial reaction rate (r_o) by approximating the tangent to the concentration time-curve (*35*); therefore, Eq. S5 can then be expressed as:

$$log\ r_o = log\,k_{obs} + \propto log\ [RDX]_o \qquad \text{[Eq. S8]}$$

Second-order rates (k) were then derived from pseudo first-order rates (k_{obs}) by the relationship in Eq. S6.

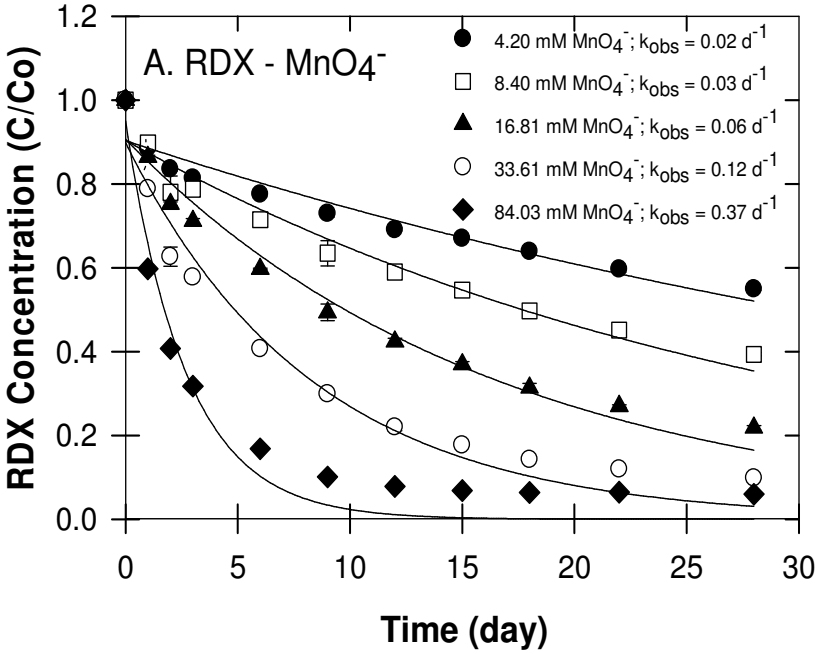

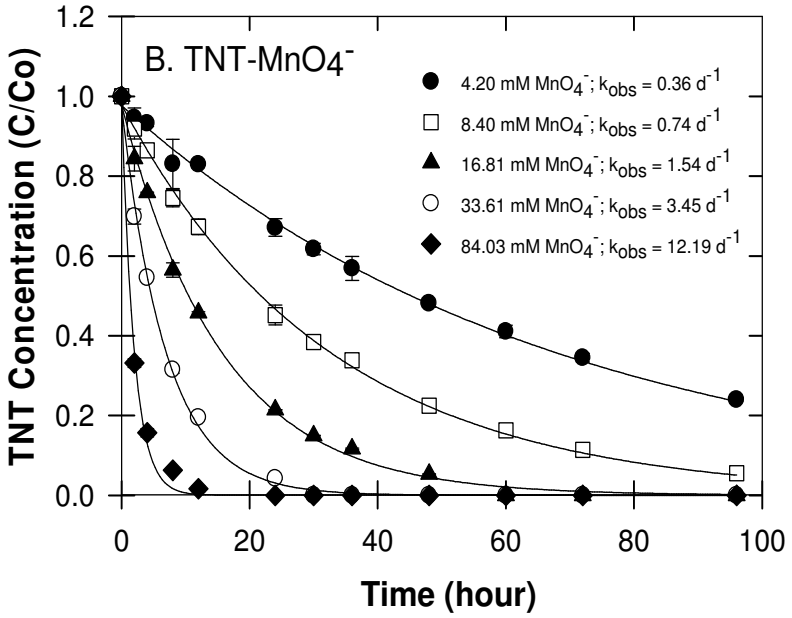

Figure S11: Loss of RDX (A) and TNT (B) when treated with various concentrations of MnO_4^-. Note differences in time scales. Bars indicate sample standard deviations (n = 3).

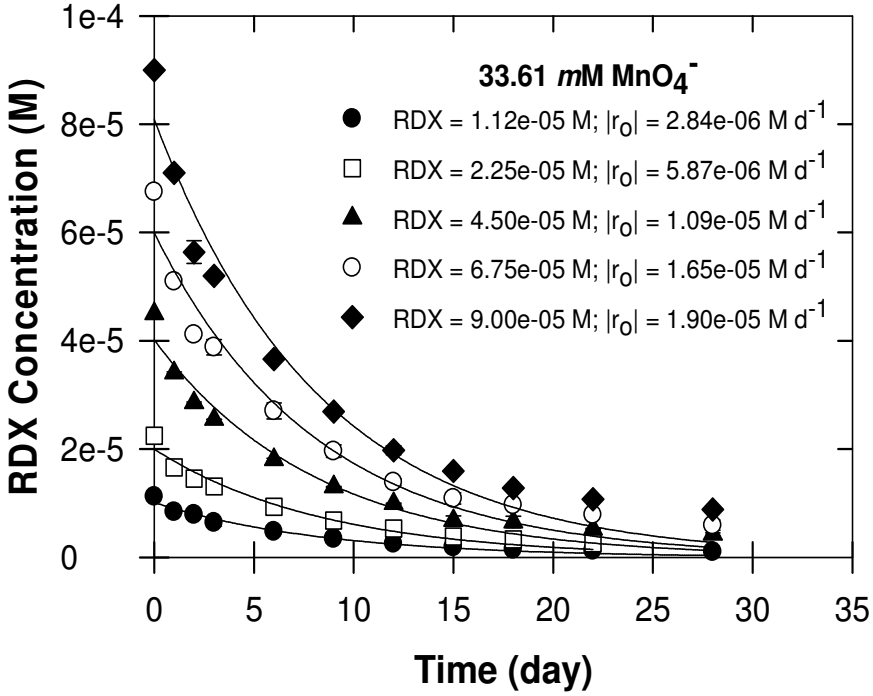

Figure S12: Loss of RDX (initial concentrations ranging from 0.01 to 0.09 *m*M) when treated with MnO_4^- at 33.61 *m*M. Bars indicate sample standard deviations (n = 3).

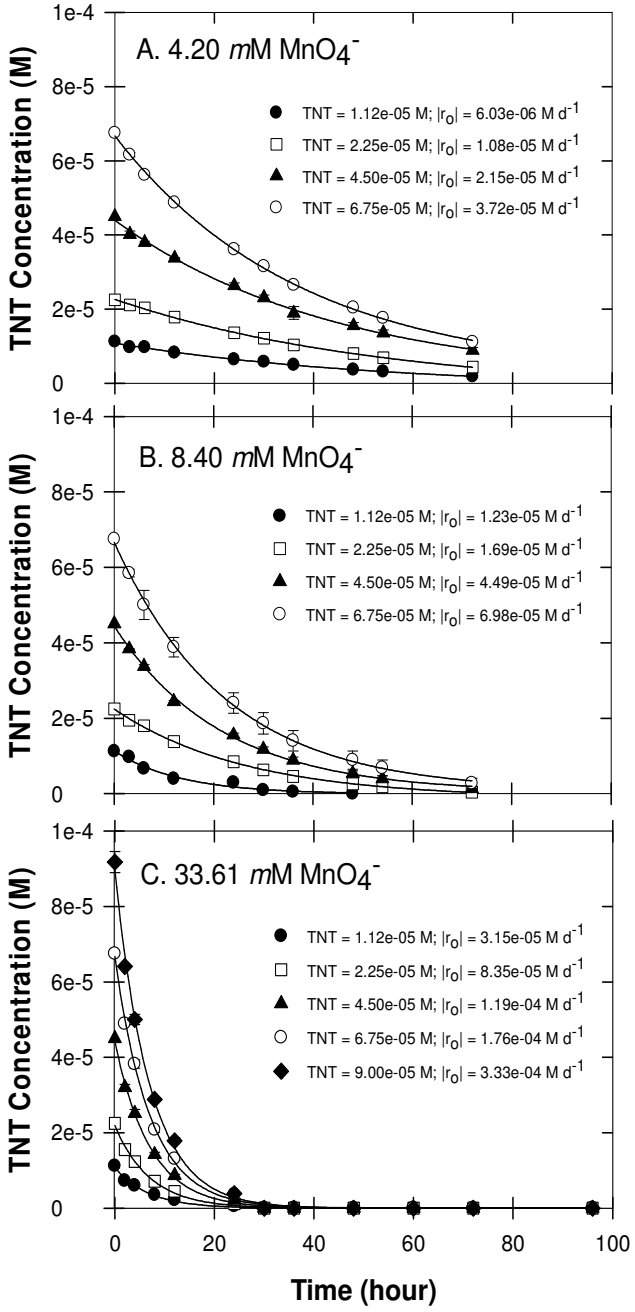

Figure S13: Loss of TNT (initial concentrations ranging from 0.01 to 0.09 *m*M) when treated with MnO_4^- at 4.20 (A), 8.40 (B), or 33.61 *m*M (C). Bars indicate sample standard deviations (n = 3).

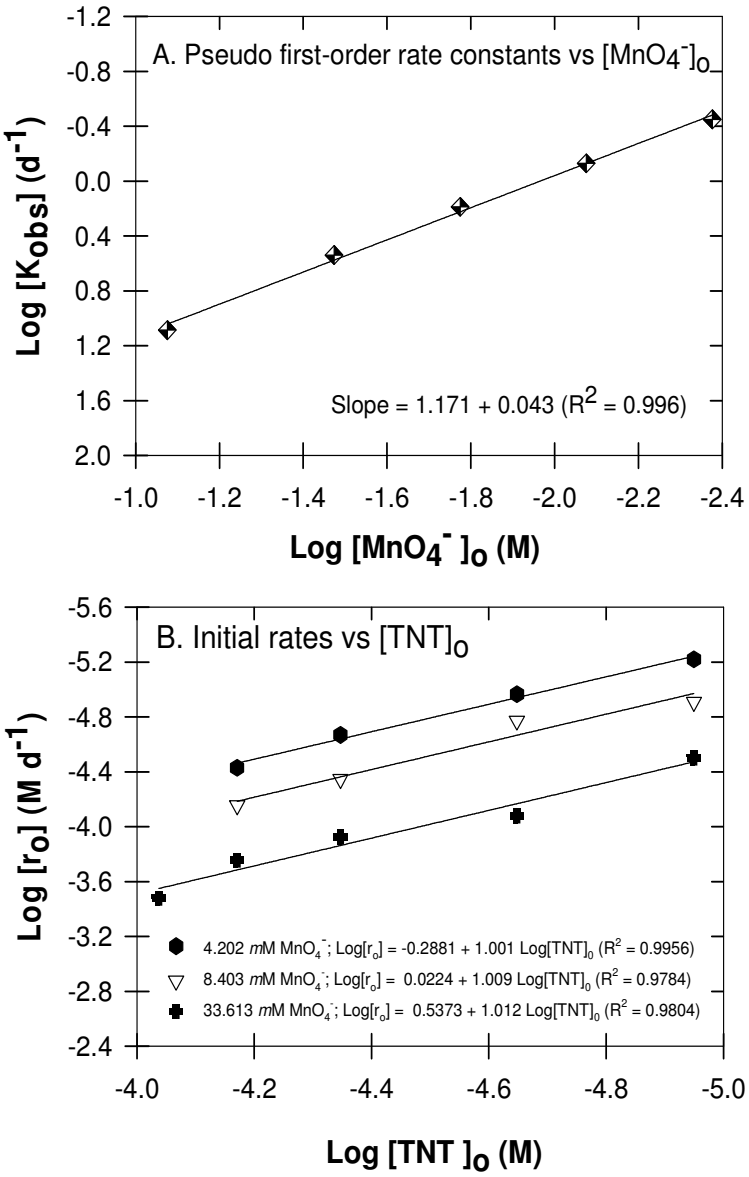

Figure S14: (A) Plot of pseudo first-order rate constants for TNT degradation vs $[MnO_4^-]$. Aqueous TNT (0.09 *m*M) was treated with MnO_4^- ranging from 4.20 to 84.03 *m*M. (B) Plot of initial rates of TNT degradation vs. $[TNT]_o$ ranging from 0.01 to 0.09 *m*M when treated with 4.20, 8.40, or 33.61 *m*M MnO_4^-.

SI-7. Temperature dependency

In RDX-MnO_4^- temperature experiment, the pseudo first-order rates were evaluated at four different temperatures. The activation energy, E, can be determined using a plot of the Arrhenius equation, as follows:

$$ln\ k\ (T) = ln\ A - \frac{E}{RT} \qquad \text{[Eq. S9]}$$

Where A is the empirical Arrhenius factor or pre-exponential factor; R is gas constant (8.314 J/K·mol); and T is the absolute temperature (K). The logarithm of the second-order rate constants (k) are plotted against the reciprocal temperature (1/T) to determine the Arrhenius factor A and the E/R value from its linear least-squares fit (*20, 36-37*).

712

713

714 **Table S2.** Temperature Dependency of Kinetic Rates for Treatment of 0.02 *m*M RDX

715 with 4.20 *m*M MnO_4^-

716

T	k_{RDX1} [a]	k_{RDX2} [a, b]	k_{RDX2} [a]	Ln k_{RDX2} [a]	1/T
(°C)	(d^{-1})	(L mol^{-1} d^{-1})	(L mol^{-1} min^{-1})		(1/K)
20	0.02	3.52	0.00	-6.01	0.0034
	(0.00)	(0.13)	(0.00)	(0.04)	
35	0.06	14.22	0.01	-4.62	0.0032
	(0.00)	(0.21)	(0.00)	(0.01)	
50	0.35	84.21	0.06	-2.84	0.0031
	(0.01)	(2.22)	(0.00)	(0.03)	
65	0.89	212.65	0.15	-1.91	0.0030
	(0.03)	(7.16)	(0.01)	(0.03)	

717

718 *a* Parenthetic values represent standard error of estimates. *b* $k_{RDX2} = k_{RDX1}/C_{MnO4-}$

719

720

721

SI-8. Single electron transfer versus hydride (or hydrogen atom) removal

Based on supporting literature (*38-40*), two key ideas emerge:

1) Two different mechanisms are observed in amino oxidations

a) single-electron transfer (SET) at the amine nitrogen and

b) hydride (or hydrogen) abstraction from the carbon;

2) The electron density on the amine nitrogen determines the operative mechanism.

Specifically, electron-poor amines or those with resonance stabilized intermediates tend to be oxidized by hydride abstraction. When these specific principles and the principles of organic oxidation chemistry are applied to RDX, the problem simplifies somewhat. For instance, there are only four distinct sites for oxidation of RDX: an oxygen atom, a nitro nitrogen atom, an amine nitrogen atom, or a carbon. This is illustrated below.

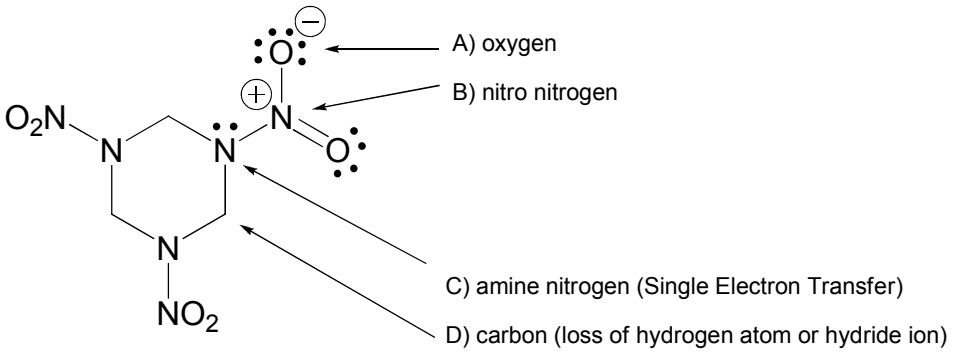

Figure S15: Possible sites for oxidation of RDX.

Oxidation at the oxygen atom or a nitro nitrogen atom would give extremely unstable intermediates since they place positive charge on electronegative oxygen or

an already electron deficient nitro group nitrogen, respectively. The only two reasonable sites for oxidation of RDX remaining are the exact two options carefully studied by the cited authors (38-40). That is, oxidation at the amine nitrogen (by SET) or oxidation at the carbon (by hydride abstraction, see S16, S17 below).

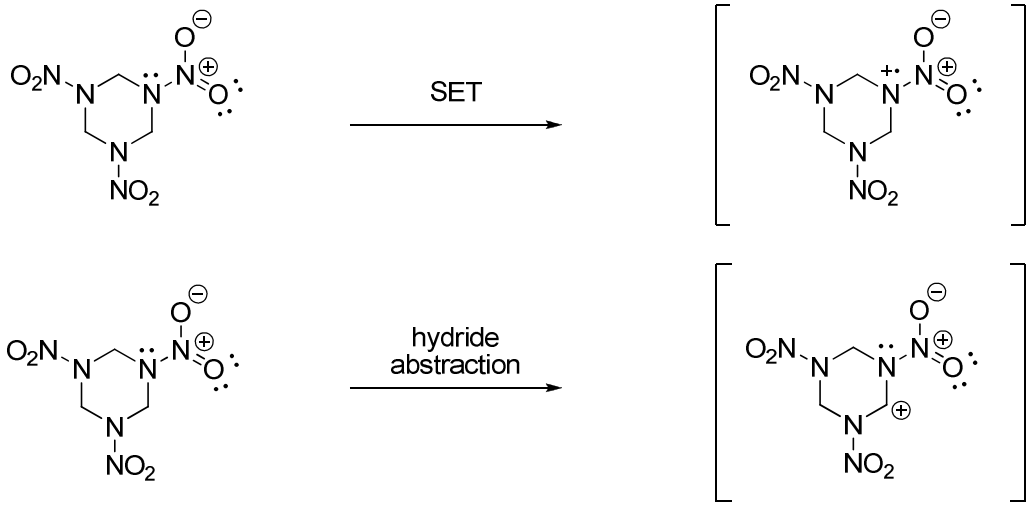

Figure S16: Overall comparison of SET versus hydride abstraction of RDX.

Because the amino nitrogens in RDX are extremely electron-poor, the hydride loss will tend to dominate the reaction. This is probably because the intermediate resulting from an initial single-electron transfer would produce an intermediate having two positive charges on the adjacent nitrogen atoms, as shown above. Such an intermediate would be much less stable than the proposed carbocation which maximizes the distance of the two positive charges from each other, and places one of them on the more electropositive carbon atom.

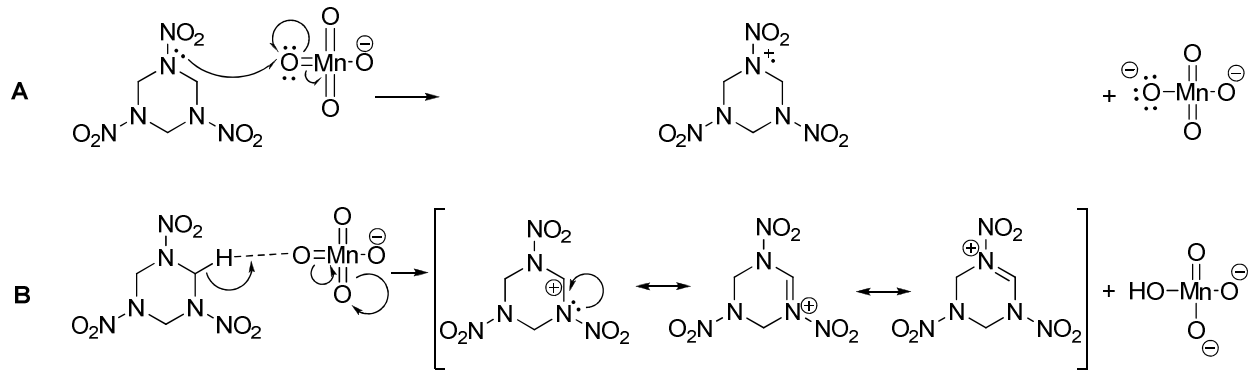

Figure S17: A comparison of initial first steps via single electron transfer (A) versus hydride removal (B).

When we considered both possible first-steps in the RDX-MnO_4^- reaction (SET vs. Hydride loss, Fig. S15), we believe the strongly electron-withdrawing nitro groups would tend to destabilize any cation intermediate. This destabilizing effect, however, would be minimized for the carbocation intermediate formed via hydride abstraction (Fig S17B) compared to the aminium ion formed by SET (Fig. S17A) because: 1) the carbocation is further from the nitro group than the aminium ion and is therefore less destabilized by inductive effects, 2) carbon is more electropositive than nitrogen, and thus less destabilized by the cation, 3) resonance stabilization for the carbocation can occur but is completely absent for the aminium intermediate. These theoretical explanations are supported by the experimental observations that 1°, 2° and 3° alkylamines having all their electron density isolated on the nitrogen tend to be oxidized by SET (*38-39*), while amines with resonance distributed electron density like benzylamine clearly undergo loss of hydride (or hydrogen atom) (*40*). Thus, theory and experiment indicate that the carbocation intermediate will be more stable and therefore formed more quickly than the aminium cation intermediate in RDX.

SI-9. Proposed RDX degradation via proton abstraction

RDX - MnO_4^- (hydrolysis and oxidation)

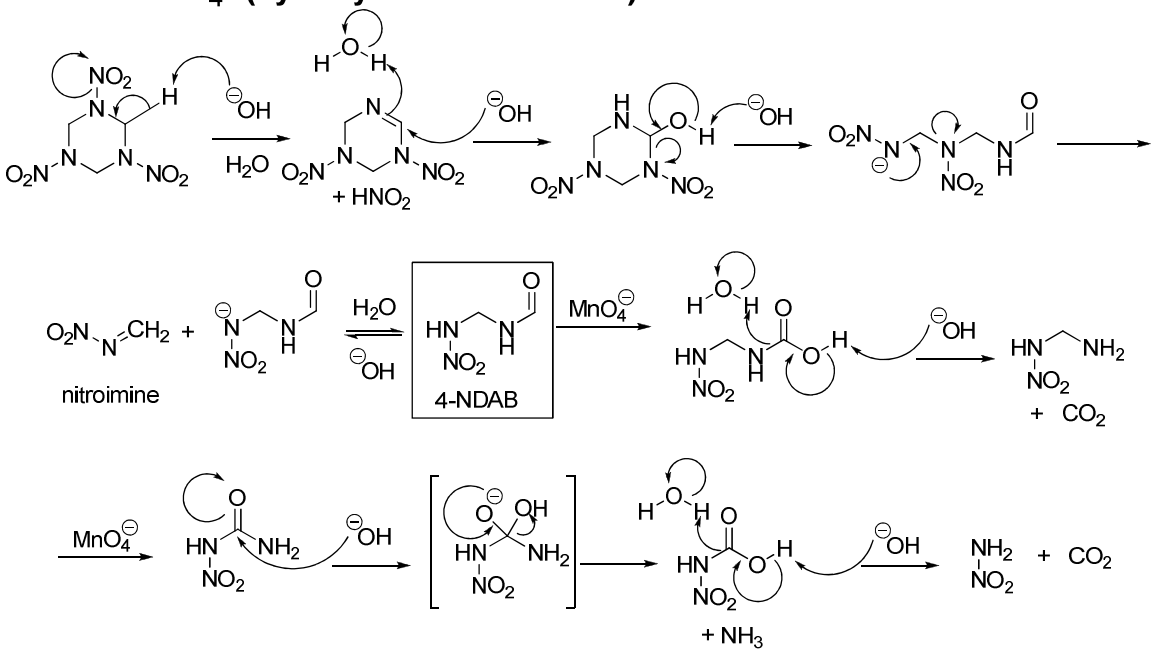

Nitroimine - MnO_4^- (hydrolysis and oxidation)

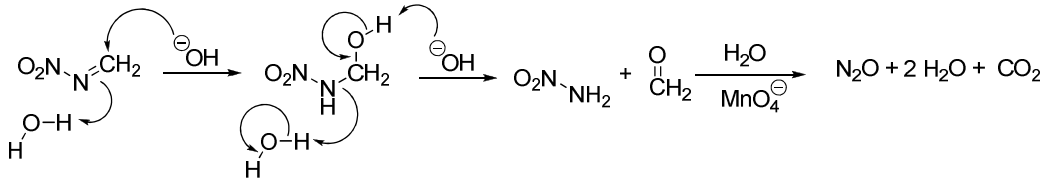

Overall reaction (HNO_2 further oxidized to HNO_3)

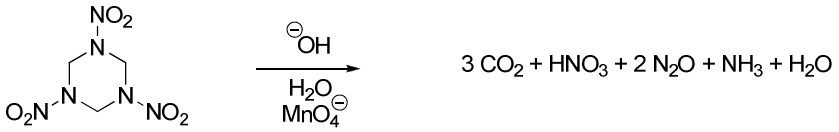

Figure S18: Proposed RDX degradation via proton abstraction and oxidation via MnO_4^- under alkaline pH.

SI-10. References

(1) Ross, P.J.; Martin, A.E. A rapid procedure for preparing gas samples for nitrogen-15 determination. *Analyst* **1970**, *95*(1134), 817-822.

(2) Sada, E.; Kumazawa, H.; Hayakawa, N. Absorption of NO in aqueous solutions of $KMnO_4$. *Chem. Eng. Sci*. **1977**, *32*(10), 1171-1175.

(3) Brogren, C.; Karlsson, H.T.; Bjerle, I. Absorption of NO in an alkaline solution of $KMnO_4$. *Chem. Eng. Technol*. **1997**, *20*(6), 396-402.

(4) Xianshe, F.; John, I.; Paula, T. Scavenging of nitric oxide and nitrogen dioxide by reactive absorption. *Fluid/Part. Sep. J*. **2003**, *15*(2), 171-174.

(5) Nelson, D.W.; Bremner, J.M. Gaseous products of nitrite decomposition in soils. *Soil. Biol. Biochem*. **1970**, *2*(3), 203-215.

(6) Tedesco, M.J.; Keeney, D.R. Determination of (nitrate+nitrite)-N in alkaline permanganate solutions. *Commun. Soil. Sci. Plant Anal*. **1972**, *3*(4), 339-344.

(7) Bundy, L.G.; Bremner, J.M. Determination of ammonium-N and nitrate-N in acid permanganate solution used to absorb ammonia, nitric oxide, and nitrogen dioxide evolved from soils. *Commun. Soil Sci. Plant Anal*. **1973**, *4*(3), 179-184.

(8) Smith, C.J.; Chalk, P.M. Determination of nitrogenous gases evolved from soild in closed systems. *Analyst* **1979**, *104*(1239), 538-544.

(9) Flasarova, M.; Novak, J.; Ulrich, R.; Vyhlidka, P. Determination of nitrites in mixtures with nitrates by using a nitrate-selective electrode. *Chem. Listy* **1986**, *80*(3), 328-331.

(10) Perez-Benito, F.J.; Arias, C.; Brillas, E. A kinetic study of the autocatalytic permanganate oxidation of formic acid. *Int. J. Chem. Kinet*. **1990**, *22*(3), 261-287.

(11) Root, D.K. In-situ chemical oxidation of chlorinated hydrocarbons in the presence of radionuclides. Presented at WM'03 Conference [Online], Tucson, AZ,

February 23-27, 2003. WM Symposia Website. http://www.wmsym.org/archives/2003/pdfs/184.pdf (accessed Feb 25, 2008).

(12) Adam, M.L.; Comfort, S.D.; Snow, D.D. Remediating RDX-contaminated ground water with permanganate: Laboratory investigations for the Pantex perched aquifer. *J. Environ. Qual.* **2004**, *33*(6), 2165-2173.

(13) Adam, M.L.; Comfort, S.D.; Snow, D.D.; Cassada, D.; Morley, M.C.; Clayton, W. Evaluating ozone as a remedial treatment for removing RDX from unsaturated soils. *J. Environ. Eng*. **2006**, *132*(12), 1580-1588.

(14) Ladbury, J.W.; Cullis, C.F. Kinetics and mechanism of oxidation by permanganate. *Chem. Rev*. **1958**, *58*(2), 403-438.

(15) Kanungo, S.B.; Parida, K.M.; Sant, B.R. Studies on MnO_2-III. The Kinetics and the mechanism for the catalytic decomposition of H_2O_2 over different crystalline modifications of MnO_2. *Electrochim. Acta* **1981**, *26*(8), 1157-1167.

(16) Lee, J.Y. Method for reductive degradation of chlorinated organic compounds using a reductive intermediate produced by decomposition of hydrogen peroxide under the existence of a manganese oxide catalyst. Korean Patent 036875. 2006.

(17) Shah, M.M. Method for digesting a nitro-bearing explosive compound. U.S. Patent 6,118,039. September 12, 2000.

(18) Zhang, W.; Zhang, Y.; Yang, Z.; Hu, L.; Ye, L. Study on decomposition of methylene blue in the presence of H_2O_2 with nanostructured Mn_2O_3 as catalysts. *Hefei Gongye Daxue Xuebao, Ziran Kexueban*. **2005**, *28*(11), 1435-1439.

(19) Gates-Anderson, D.D.; Siegrist, R.L.; Cline, S.R. Comparison of potassium permanganate and hydrogen peroxide as chemical oxidants for organically contaminated soils. *J. Environ. Eng*. **2001**, *127*(4), 337-347.

(20) Heilmann, H.M.; Wiesmann, U.; Stenstrom, M.K. Kinetics of the alkaline

842 hydrolysis of high explosives RDX and HMX in aqueous solution and adsorbed to
843 activated carbon. *Environ. Sci. Technol*. **1996**, *30*(5), 1485-1492.
844 (21) Jackson, R.G.; Rylott, E.L.; Fournier, D.; Hawari, J.; Bruce, N.C. Exploring the
845 biochemical properties and remediation applications of the unusual explosive-
846 degrading P450 system XplA/B. *Proc. Natl. Acad. Sci. USA*. **2007**, *104*(43),
847 16822-16827.
848 (22) Suthersan S.; Ganczarcczyk, J. Inhibition of nitrite oxidation during nitrification.
849 *Water Pollut. Res*. **1986**, *21*(2), 257-266.
850 (23) Cleemput, O.V.; Samater, A.H. Nitrite in soils: Accumulation and role in the
851 formation of gaseous N compounds. *Fert. Res.* **1996**, *45*(1), 81-89.
852 (24) Balakrishnan, V.K.; Halasz, A.; Hawari, J. Alkaline hydrolysis of the cyclic
853 nitramine explosives RDX, HMX, and CL-20: New insights into the degradation
854 pathyways obtained by the observation of novel intermediates. *Environ. Sci.*
855 *Technol.* **2003**, *37*(9), 1838-1843.
856 (25) Chokejaroenrat, C. Laboratory and pilot-scale investigations of RDX treatment by
857 permanganate. M.S. Thesis, University of Nebraska-Lincoln, Lincoln, NE, 2008.
858 (26) Yan, Y.E.; Schwartz, F.W. Kinetics and mechanisms for TCE oxidation by
859 permanganate. *Environ. Sci. Technol*. **2000,** *34*(12), 2535-2541.
860 (27) Li, Z.M.; Comfort, S.D.; Shea, P.J. Destruction of 2,4,6-trinitrotoluene (TNT) by
861 Fenton oxidation. *J. Environ. Qual*. **1997**, *26*(2), 480-487.
862 (28) Yan, Y.E.; Schwartz, F.W. Oxidative degradation and kinetics of chlorinated
863 ethylenes by potassium permanganate. *J. Contam. Hydrol.* **1999,** *37*(3-4), 343-
864 365.
865 (29) Huang, K.; Hoag, G.A.; Chheda, P.; Woody, B.A.; Dobbs, G.M. Kinetic study of
866 oxidation of trichloroethylene by potassium permanganate. *Environ. Eng. Sci*.
867 **1999**, *16*(4), 265-274.

(30) Huang, K.; Hoag, G.A.; Chheda, P.; Woody, B.A.; Dobbs, G.M. Oxidation of chlorinated ethenes by potassium permanganate: A kinetics study. *J. Hazard. Mater*. **2001**, *87*(1-3), 155-169.

(31) Siegrist, R.L.; Urynowicz, M.A.; West, O.A.; Crimi, M.L.; Lowe, K.S. *Principles and practices of in-situ chemical oxidation using permanganate*; Battelle Press: Columbus, OH, 2001.

(32) Waldemer, R.H.; Tratnyek, P.G. Kinetics of contaminant degradation by permanganate. *Environ. Sci. Technol*. **2006**, *40*(3), 1055-1061.

(33) Siegrist, R.L.; Urynowicz, M.A.; Crimi, M.L.; Lowe, K.S. Genesis and effects of particles produced during in-situ chemical oxidation using permanganate. *J. Environ. Eng*. **2002**, *128*(11), 1068-1079.

(34) SPSS. SigmaPlot for Windows Version 10.0: Chicago, IL, 2006.

(35) Casado, J.; Lopez-Quintela, M.A.; Lorenzo-Barral, F.M. The initial rate method in chemical kinetics: Evaluation and experimental illustration. *J. Chem. Educ.* **1986**, *63*(5), 450-452.

(36) Karakaya, P.; Mohammed, S.; Christos, C.; Steve, N.; Wendy, B. Aqueous solubility and alkaline hydrolysis of the novel high explosive hexanitrohexaazaisowurtzitane (CL-20). *J. Hazard. Mater*. **2005**, *120*(1-3), 183-191.

(37) Benson, S.W. *The Foundations of chemical kinetics*; Krieger Publishing Co.: Florida, 1982; pp 66-68.

(38) Rosenblatt, D.H.; Davis, G.T.; Hull, L.A.; Forberg, G.D. Oxidations of amines. V. Duality of mechanism in the reactions of aliphatic amines with permanganate *J. Org. Chem.* **1968**, *33*(4), 1649-1650.

(39) Mata-Perez, F.; Perez-Benito, J.F. Kinetics and mechanisms of oxidation of methylamine by permanganate ion. *Can. J. Chem.* **1987**, *65*(10), 2373-2379.

(40) Wei, M.; Stewart, R. The mechanisms of permanganate oxidation. VIII. Substituted benzylamines *J. Am. Chem. Soc.* **1966**, *88*(9), 1974-1979.